

Solar Photodecomposition for Removing BTEX Compounds from Groundwater Contaminated by Gasoline Station Activities

Priscila Moreira Peres Garcia , Nilce Ortiz

Center for Environmental Chemistry, Nuclear and Energy Research Institute—IPEN-CNEN, São Paulo, Brazil
Email: priscila.garcia1008@gmail.com

How to cite this paper: Garcia, P. M. P., & Ortiz, N. (2025). Solar Photodecomposition for Removing BTEX Compounds from Groundwater Contaminated by Gasoline Station Activities. *Journal of Geoscience and Environment Protection*, 13, 325-346.
<https://doi.org/10.4236/gep.2025.133018>

Received: December 24, 2024

Accepted: March 22, 2025

Published: March 25, 2025

Copyright © 2025 by author(s) and Scientific Research Publishing Inc.
This work is licensed under the Creative Commons Attribution-NonCommercial International License (CC BY-NC 4.0).
<http://creativecommons.org/licenses/by-nc/4.0/>



Open Access

Abstract

The study investigates the application of solar photodecomposition to remove BTEX compounds (benzene, toluene, ethylbenzene, and xylenes) from groundwater contaminated by gasoline station activities. BTEX compounds, known for their toxicity and carcinogenicity, pose significant environmental and public health risks. The primary goal of this research was to develop effective and sustainable technology for treating and removing BTEX from groundwater using solar photodecomposition. To achieve this objective, microstructured titanium dioxide (TiO₂) was combined with diatomite to leverage heterogeneous photocatalysis for BTEX degradation. The TiO₂-Diatomite (TiO₂-Dt) composite was characterized using scanning electron microscopy (SEM) and thermogravimetric analysis (TGA). SEM provided detailed insights into the material's structure and morphology, while TGA assessed the thermal stability of the photocatalyst in BTEX degradation processes. Experimental results demonstrated that solar photodecomposition is an effective method for water remediation. Tests conducted with 9.0 g of TiO₂-Dt and 40% BTEX solutions evaluated the removal efficiency across varying catalyst masses (0.8 g to 2.5 g). The highest BTEX removal efficiency, 79.0%, was achieved with 1.0 g of TiO₂-Dt. Catalyst amounts between 1.0 g and 1.2 g showed good performance, with removal efficiencies ranging from 71.4% to 79.0%. However, increasing the catalyst mass to 2.0 g and 2.5 g resulted in reduced efficiencies (57.4% to 64.4%), suggesting saturation or dispersion limitations. Breakthrough curves and Boltzmann calculations confirmed TiO₂-Dt's effectiveness in solar photodecomposition. Moderate catalyst amounts (1.0 - 1.2 g) optimized BTEX removal, while higher quantities reduced efficiency, underscoring solar radiation's role in accelerating pollutant degradation.

Keywords

Solar Photodecomposition, BTEX, Groundwater, Titanium Dioxide,

1. Introduction

The commercialization of petroleum-derived fuels has led to releasing mono-aromatic hydrocarbons such as benzene, toluene, ethylbenzene, and xylenes (BTEX), significant pollutants. These compounds frequently contaminate groundwater and surface water through various sources, including the disposal of industrial effluents, leaking gas station tanks, and road accidents. Managing contaminated sites effectively is crucial for mitigating water contamination risks and protecting human health. The study involves understanding the site's characteristics and the impacts of contaminants, which aids in making informed decisions about intervention strategies and appropriate mitigation measures (ANP, 2021).

Despite the well-documented health risks associated with BTEX compounds, groundwater contamination by these substances is often overlooked and remains untreated in many municipal systems. This neglect increases the risk of water-borne diseases for communities relying on contaminated supply wells.

BTEX compounds are often overlooked in remediation efforts due to their subtle presence in water, complicating analysis compared to polycyclic aromatic hydrocarbons (PAHs). Despite their low visibility in environmental monitoring, BTEX compounds are prevalent and can be found in various sources, including petrochemical industry waste, streams, domestic waste, municipal landfills, and groundwater plumes, sometimes far from the original spill sites. Research, such as that by (Andrade et al., 2010), has detected BTEX compounds in drinking water, highlighting significant health risks.

Several remediation techniques have addressed BTEX contamination, particularly at spill sites. Bioremediation and natural attenuation are among the most commonly used methods. However, these techniques often face challenges due to the extended time required for effective implementation and the difficulty meeting stringent water quality standards.

Government regulatory agencies have reported a rising number of contaminated sites associated with gas stations, as evidenced by environmental inventories conducted in Brazilian states such as São Paulo and Minas Gerais (CETESB, 2014). This increase corresponds with the implementation of CONAMA Resolution No. 273/2000 (CONAMA 273, 2000), which mandates the investigation of environmental liabilities for gas stations as part of the environmental licensing process. As concerns over surface and groundwater quality grow, developing effective technologies for treating and removing BTEX compounds becomes increasingly vital.

CONAMA Resolution No. 420/2009 (CONAMA 420, 2009) outlines the procedures for managing contaminated areas. It sets criteria and guiding values for soil quality, prevention, and groundwater investigation. The resolution also stipulates

that if the identified chemical substances pose risks to human health and the environment, the responsible agencies must undertake specific actions to safeguard affected populations.

Contaminated areas have been a persistent concern for public managers, with the State of São Paulo leading in the identification and documentation of these sites. Since 2002, the Environmental Company of the State of São Paulo (CETESB), affiliated with the State Secretariat for the environment, has been conducting inventories to track and report contaminated areas (**Figure 1**). These reports reveal that gas stations are the primary contributors to soil and groundwater contamination in the state, accounting for 3.82 cases (74%). These numbers significantly surpass other sources, such as industrial activities (17%), commercial operations (5%), waste disposal facilities (3%), and miscellaneous sources, including accidents, agriculture, and unknown origins (1%) (CETESB, 2021).

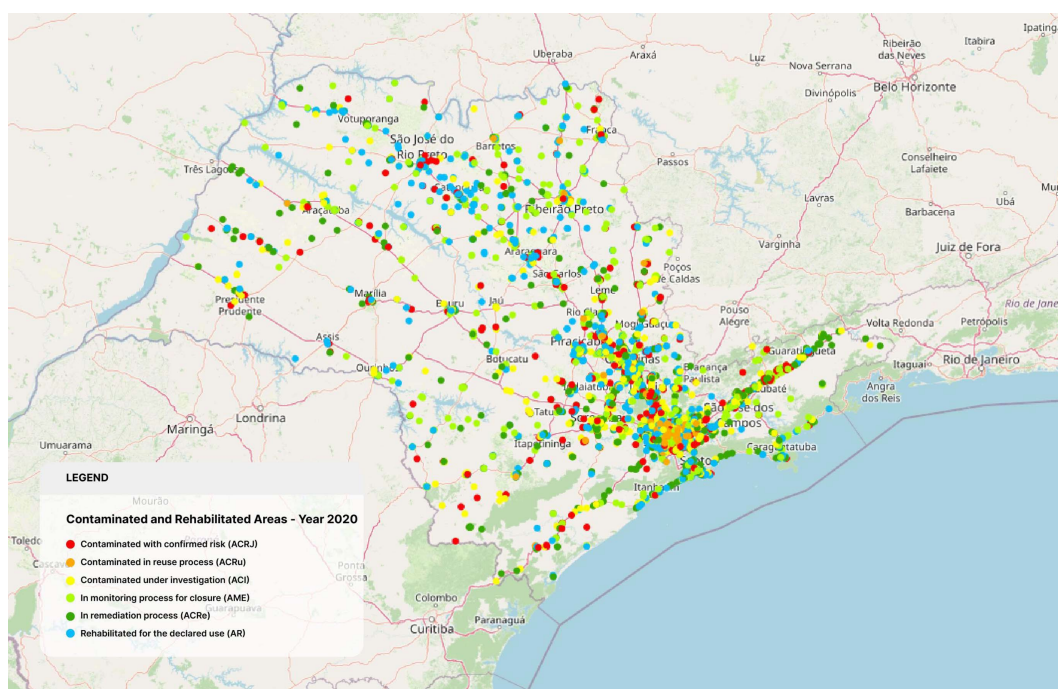


Figure 1. Map of contaminated and rehabilitated areas. Source: DATAGEO, 2021.

The heightened focus on areas contaminated by petroleum-derived compounds drives by the complexity, toxicity, and environmental mobility of mono-aromatic compounds in the BTEX group (Benzene, Toluene, Ethylbenzene, and Xylenes). These compounds are highly toxic to both the environment and human health, acting as central nervous system depressants and exhibiting greater chronic toxicity than aliphatic hydrocarbons (also found in petroleum products), even at concentrations as low as $\mu\text{g/L}$ (Andrade et al., 2010).

Given the identification of automotive fuel stations as the major source of soil and groundwater contamination in the states mentioned (**Figure 2**), it is crucial for environmental control agencies in other regions to prioritize and address this

issue with the same level of attention.

The primary objective of this study is to provide an overview of gas stations contributing to soil and groundwater contamination in the city of São Paulo. The research achieved through a documentary analysis of the environmental licensing processes for gas stations held by the State Secretariat for the Environment (SEMA/SP). The study emphasizes the critical need for comprehensive inventorying of these contaminated areas to implement appropriate remediation measures. Additionally, it highlights the significant potential for fuel stations to contaminate soil and groundwater, which can limit the usability of nearby wells for public water supply.

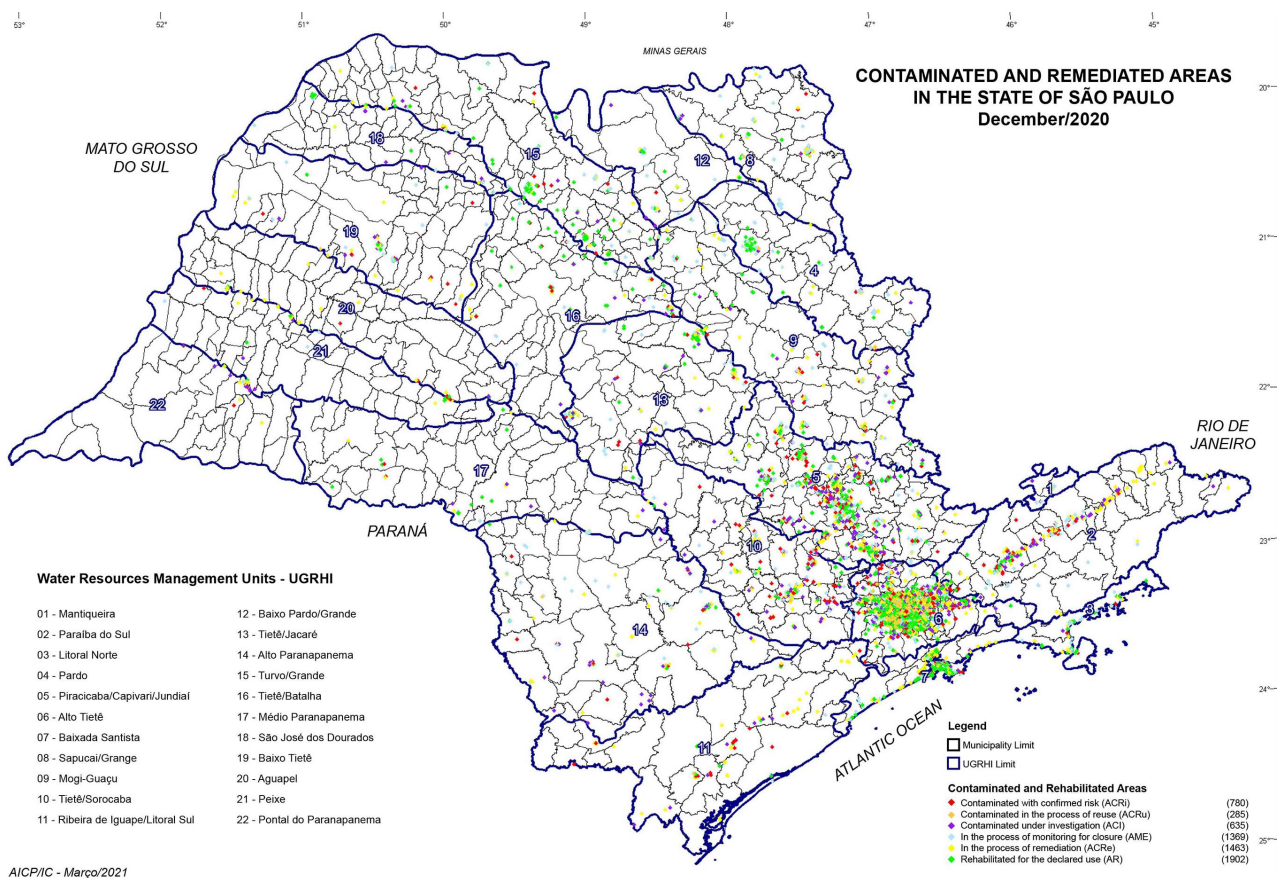


Figure 2. Map showing the gas station distribution and contaminated areas. Source: CETESB, 2021.

The study's second phase was the treatment of some synthetic water samples contaminated with BTEX using photodecomposition processes. The gasoline content in these synthetic water samples was equivalent to the levels reported by environmental agencies for contaminated groundwater. The treatment utilized microstructured titanium dioxide (TiO₂) synthesized with biotemplate, a catalyst widely employed in heterogeneous photocatalysis. This approach benefits from the catalyst's ability to mineralize a broad range of organic compounds, the high efficiency of produced hydroxyl radicals, the potential for catalyst reuse, and the use

of solar radiation during the reaction and as an energy source (SURI *et al.*, 1993).

In Brazil, the application of heterogeneous solar photocatalysis is particularly well-suited due to the country's favorable solar energy conditions. The abundant solar resource makes the process viable and sustainable, leveraging renewable energy (Luiz, 1985). Solar energy is promising for meeting wastewater treatment needs through advanced oxidative processes, especially in countries with high solar insolation. Brazil's consistently high levels of global irradiation across its territory support the feasibility of solar-driven treatments.

Solar photodecomposition is an effective method for treating and degrading organic pollutants. This process primarily generates hydroxyl (HO^{*}) and superoxide (O₂^{*}) radicals, with HO^{*} as the main oxidant. TiO₂ acts as a catalyst, facilitating the production of hydroxyl radicals through a series of reactions (Ortiz *et al.*, 2021). Given the increasing concerns about groundwater quality, advancing technologies for BTEX removal using solar photodecomposition is crucial. **Table 1** shows the literature references used in this study.

Table 1. Main references of published studies on BTEX.

AUTOR	ANO	ESTUDO
DÓREA, H. S. <i>et al.</i>	2006	Analysis of BTEX, PAHs, and metals in produced water from an oil field in the state of Sergipe, Brazil.
SILVA, A. M. S; PIMENTA. M. F; JR. RAIUMUNDO. I. M; ALMEIDA. Y. M. B	2007	A PVC detection phase for BTEX determination in water using mid-infrared spectroscopy.
DÂNIA ELISA CHRISTOFOLETTI MAZZEO, SILVIA TAMIE MATSUMOTO, CARLOS EMÍLIO LEVY, DEJANIRA DE FRANCESCHI DE ANGELIS, MARIA APARECIDA MARIN-MORALES	2013	Application of cellular structures and assays to evaluate BTEX biodegradation.
MUFTAH H. EL-NAAS, JANICE A. ACIO, AYAT E. EL TELIB	2014	Aerobic BTEX biodegradation: advances and perspectives.
PATRÍCIA RACHEL FERNANDES DA COSTA, DJALMA RIBEIRO DA SILVA, CARLOS ALBERTO MARTÍNEZ-HUITLE, SERGI GARCIA-SEGURA	2015	Treatment of fuel station effluents using electrochemical technology.
KAMAL KHODAEI, HAMID REZA NASSERY, MAHNAZ MAZAHARI ASADI, HOSSEIN MOHAMMADZADEH, MOJTABA G. MAHMOODLU	2016	BTEX biodegradation in contaminated groundwater using a new strain (<i>Pseudomonas</i> sp. BTEX-30).
SANTOS, C. R. S. N	2016	Bioprocesses and bioindicators for monitoring water treatment.

Continued

RENATO NALLIN MONTAGNOLLI, PAULO RENATO MATOS LOPES, JAQUELINE MATOS CRUZ, MARINA TURINI CLARO, GABRIELA MERCURI QUITERIO, EDERIO DINO BIDOIA	2017	BTEX biodegradation induced by the presence of perfluorinated compound foams used in firefighting.
CHENG-DI DONG, MEI-LING TSAI, CHIU-WEN CHEN, CHANG-MAO HUNG	2017	Persulfate oxidation in heterogeneous catalysis of BTEX and MTBE using Fe ₃ O ₄ CB magnetite composites and the cytotoxicity of degradation products.
Z. SHEIKHOLESAMI, D. YOUSEFI KEBRIA, F. QADERI	2018	Nanoparticle for BTEX degradation in produced water: an experimental procedure.
ORTIZ, N., SILVA, A., LIMA, G. N. S., HYPPOLITO, F. P.	2021	A study on the solar photodecomposition process with TiO ₂ followed by biochar adsorption, resulting in 94% amoxicillin removal.
KOTANI, O. P.	2023	Use of TiO ₂ -Diatomite in photodisinfection processes for water contaminated by bacteria. 2023. 98 f. Dissertation (Master's in Nuclear Technology), Institute for Energy and Nuclear Research, IPEN-CNEN, São Paulo.
NA LV, XIUFEN LI.	2023	Phosphorus removal from wastewater using Ca-modified attapulgite: Fixed-bed column performance and breakthrough curves analysis.
ESLAM IBRAHIM EL-ASWAR, SABAH S. IBRAHIM, YASMEEN R. ABDALLAH, KHALED ELSHARKAWY.	2024	Removal of ciprofloxacin and heavy metals from water by bentonite/activated carbon composite: Kinetic, isotherm, thermodynamic, and breakthrough curve modeling studies
FERRO, M. D.	2024	Use of microstructured TiO ₂ with biochar for catalytic solar disinfection of effluents contaminated by microorganisms. 2024. 125 f. Dissertation (Master's in Nuclear Technology), Institute for Energy and Nuclear Research, IPEN-CNEN, São Paulo.

Source: Author.

2. Materials and Methods

2.1. Photocatalytic Mechanism

Heterogeneous catalytic reactions involve a series of physical transport steps that can influence the overall reaction rate. In photocatalytic systems, these steps occur sequentially, as described by Vazzoler (2019):

1) Initial movement of reactants or microorganisms through a boundary layer adjacent to the catalyst surface.

- 2) Internal transport within the catalyst pores, allowing the reactants to reach the active sites (intraparticle diffusion).
- 3) Interaction of reactants with the catalyst surface, leading to adsorption.
- 4) Chemical conversion at the active sites, followed by the release of products (desorption).
- 5) Transport of products within the pores, moving toward the catalyst's external surface.
- 6) Dispersion of products through the external boundary layer, enabling their release into the surrounding fluid.

The main chemical transformations associated with photocatalytic decomposition and disinfection occur during steps 3 and 4, where the catalyst's surface area plays a crucial role. However, the other steps can also affect the process's overall efficiency. Typically, the slowest step serves as the limiting factor, determining the overall reaction behavior.

The kinetic study of these systems aims to determine the rate of chemical reactions and identify the factors influencing them. For this purpose, pseudo-first-order equations (Equation 2), pseudo-second-order equations (Equation 3), and intraparticle transport equations (Equation 4) are commonly applied (Ray, Dhakal, & Lee, 2017).

2.2. Synthesis of Diatomite + TiO₂

The TiO₂-Dt semiconductor synthesis allows its use in the tests with a magnetic stirrer using a beaker containing distilled water, glacial acetic acid, titanium isopropoxide, and natural diatomite. After adding the reagents and the distilled water, complete the volume until 400 ml with the final suspension mixed for 2 to 3 hours. After decantation and filtration, the solid formed by the sol-gel process was placed in an oven heated to an average temperature of 373K for 24 hours to obtain TiO₂-Dt microstructures. The prepared material suffers a drying step, storage, and use in solar photodecomposition.

The synthesis process of microstructured TiO₂-Dt was based on the hydrolysis of titanium isopropoxide, using natural diatomite as the structural template. The catalyst preparation used the sol-gel method. In the experiments described, TiO₂-Dt samples prepared with 8.0 g and 9.0 g of natural diatomite. With these proportions of diatomite addition of 5 mL of glacial acetic acid and 10 mL of titanium isopropoxide, the final volume was 400 mL adjusted with distilled water. The final suspension was stirred for 2 hours, and after 1 hour of decantation, the solid formed was placed in an oven heated to 373K for 24 hours to obtain microstructures shaped with TiO₂-Dt. The storage of the obtained material follows the drying process (Figure 3).

2.3. Photodecomposition Processes

The tests carried out in the Center for Environmental Chemistry—CEQMA laboratory at IPEN. The parameters of the photodecomposition process studied

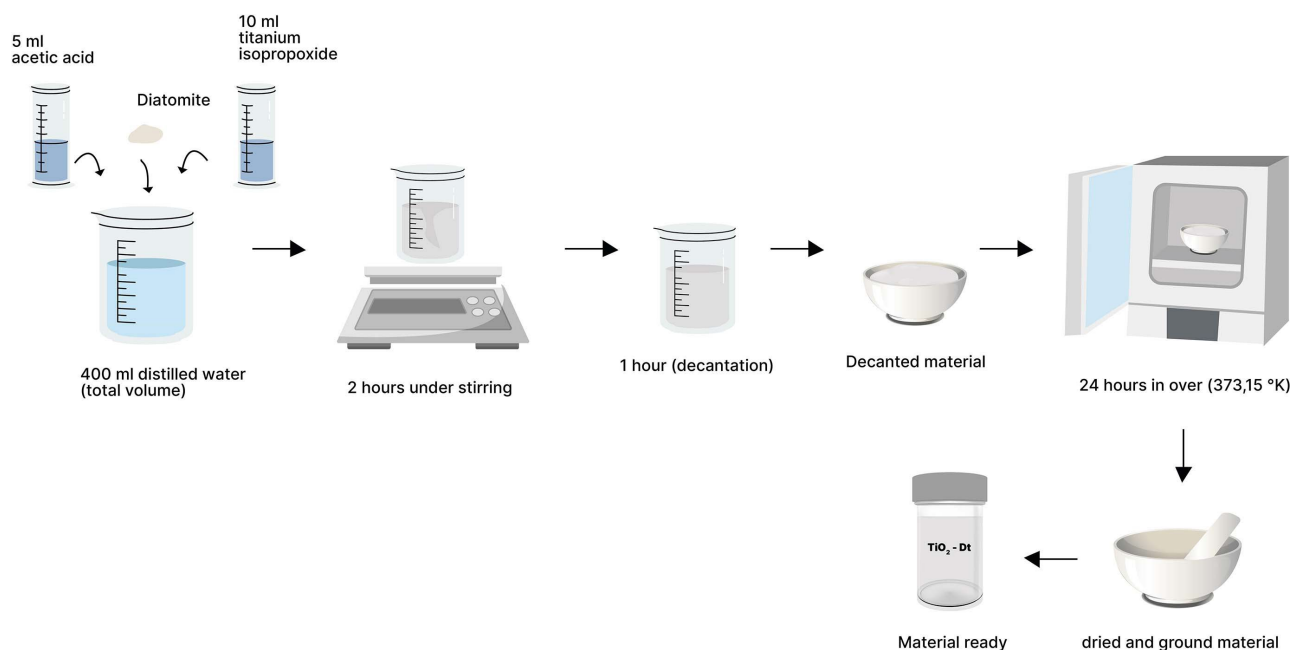


Figure 3. Steps of the TiO_2 -Diatomite synthesis process. Source: Author.

were the mass proportion 9.0 g of TiO_2 -Dt, the synthetic solutions of the water and BTEX % prepared in the laboratory, stirring time and incidence of artificial solar radiation, pH = 5.0 values, lux 380 and temperature 295 K - 298 K. The photocatalyst column filled with TiO_2 -DT had the percolation process lasting for two hours. The control of the photodecomposition process applied by the collected aliquots after percolation and the aliquot analysis allows the determination of BTEX concentrations. The column preparation was with a fixed bed of TiO_2 -Dt, and the percolation process enabled the collection of aliquots at time flow intervals of 0, 30, 60, 90, and 120 minutes for BTEX photodecomposition (**Figure 4**).

Preparing the BTEX synthetic solutions uses different volumes of gasoline purchased at the gas station commonly sold to the public. All the glassware used belongs to the CEQMA laboratory, and the acquisition of the titanium isopropoxide, acetic acid, and other reagents used were with a high level of purity and analytical grade.

Two LED lamps installed in the solar chamber simulated solar radiation, allowing solar photodecomposition to occur under controlled conditions. The BTEX solutions were prepared and diluted in different concentrations (BTEX and distilled water) at values equivalent to those found in the literature for contaminated waters.

The light chamber, designed by the author and built in the CEQMA laboratories, has the following dimensions: height of 45 cm, width of 55 cm, and depth of 55 cm. Fluorescent LED lamps were used as a source of artificial sunlight and located approximately 10 cm from the solution. The lux meter inside the light chamber measured the illuminance during the experiments. The lux measurements ranged from 380 to 390 lux.

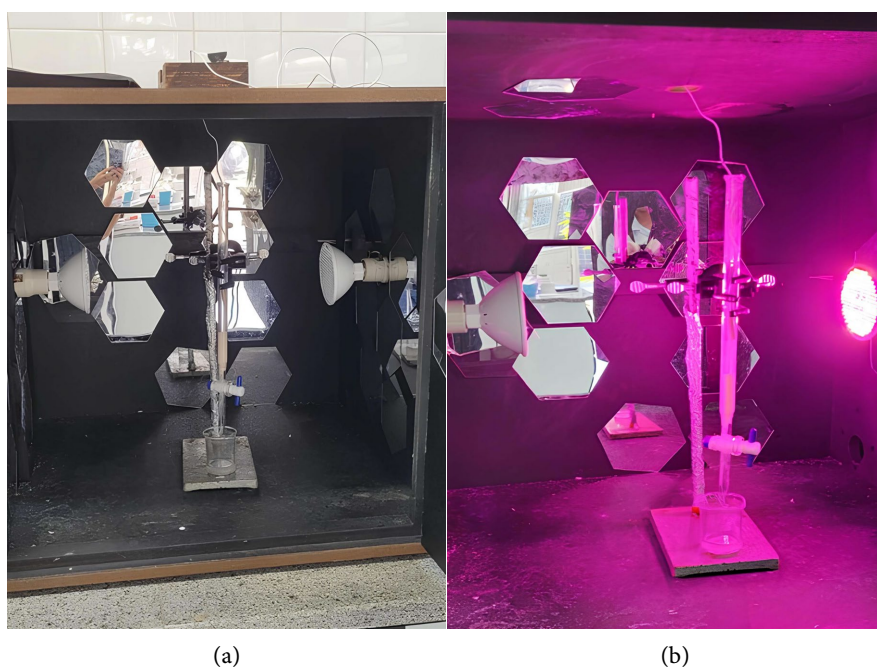


Figure 4. BTEX solution with $\text{TiO}_2\text{-Dt}$ inside the Light chamber. Source: Author.

After collecting the aliquots at different times of percolation and irradiation, the benzene content was controlled using the UV–visible spectrophotometer. **Figure 5** illustrates the spectrophotometer connected to the computer for readings and allows observing the photodecomposition process.

The ordinary gasoline purchased in most gas stations has the most common toxic substance, the BTEX mixture. This aromatic mixture has a preponderance of the benzene content, with about 70% of the total. The analytical method to measure and control the BTEX water contamination is the use of Gas Chromatography with Mass detector (CG-MS).

The use of UV-VIS spectrophotometry helps to control the photodecomposition process by determining the benzene concentration in each collected aliquot at the characteristic wavelength of $\lambda 268$ nanometers (nm).

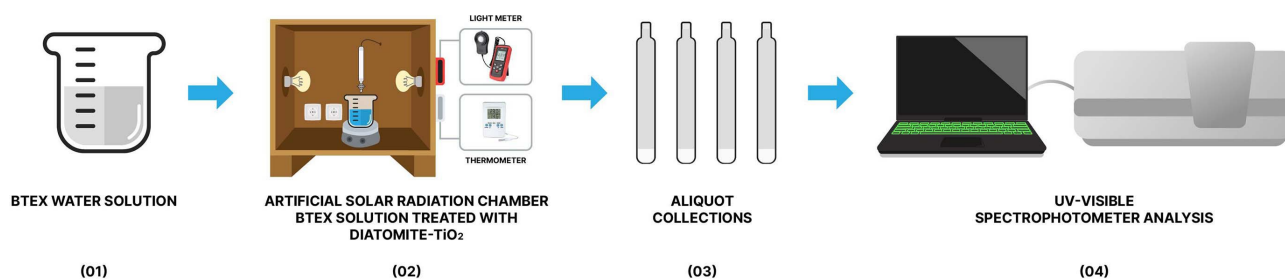


Figure 5. Photodecomposition process carried out in the laboratory. Author.

- 1—BTEX solution with $\text{TiO}_2\text{-Dt}$;
- 2—Artificial solar radiation chamber;
- 3—Aliquot collections;

4—Analysis with UV-visible spectrophotometer.

2.4. UV-VIS Spectrometry

The spectrophotometry principle is that each compound absorbs or transmits light at specific wavelengths. This relationship allows determining a compound's concentration based on the amount of light absorbed or transmitted.

In essence, the technique leverages the interaction of light with matter to measure concentration. Every chemical compound absorbs, transmits, or reflects light within a particular wavelength range. Spectrophotometry quantifies the concentration of compounds in a solution by measuring the extent to which they absorb or transmit light. The amount of light absorbed or transmitted is directly proportional to the concentration of the substance in the solution (Dias et al., 2016).

In this study, spectrometry was used to measure and control the photodecomposition process by measuring the absorbance of the benzene compound.

2.5. Gas Chromatography GC-MS

For the BTEX analysis using the equipment Shimadzu 17A gas chromatograph Kyoto -Japan allows the quantification of the organic compound content. The photoionization equipment and flame ionization detectors, with a split/splitless injector. A DB-624 megabore fused silica column (6% cyanopropylphenyl-94% dimethylpolysiloxane; 75 m × 0.53 mm ID, 3 μm), supplied by J&W Scientific (Folsom, CA, USA), was used. The carrier gas, helium, with a purity of 99.99%, was maintained at a flow rate of 10 mL/min.

During the process, the column temperature program was carefully controlled: initially, the temperature was set to 303 K for 1 minute, followed by an increase to 372 K at a rate of 278 K/min. Subsequently, a direct rise to 493 K at a 281 K/min rate occurred, maintaining at 493 K for 5 minutes. The injection port and detector temperatures were set at 453 K and 493 K, respectively. The PID system was operated with a 10 eV lamp and an intensity of 1 mA, as described by Dórea et al. (2006).

Additionally, the GC-MS chromatography technique enabled the identification of the organic composition of the analyzed samples. This approach provided a detailed characterization of the compounds separated in different retention times; afterward, the sample has the content confirmation by the fragmentogram obtained in the Mass detector.

3. Results and Discussion

During the research, the experiments conducted were in a controlled laboratory environment. Initial photodecomposition tests aimed to investigate the effects of variations in the initial concentrations of BTEX, the impact of adding different amounts of diatomite (TiO₂), and the variation of temperature within the range of 298 K to 313 K.

The choice of test temperatures considered the typical conditions of direct solar exposure found in tropical regions. Generally, photodecomposition processes are feasible at temperatures between 293 and 353 K, with values below or above this range potentially significantly influencing the efficiency of organic compound removal (Buth, 2009).

The trials with adding biochar as a biotemplate in the catalyzer synthesis were less satisfactory than expected, as the material had such small granularity that it passed into the aqueous BTEX solution. Therefore, we sought another material that also responds well to photodecomposition, which is diatomite, and it showed the first indications of satisfactory results. However, the excessive use of diatomite mass turns the suspension dense and shows interference with the absorption of solar and UV rays, hindering the photodecomposition process. This interference indicates the importance of finding an appropriate balance in the amount of diatomite used to optimize the efficiency of the contaminant removal process.

3.1. The Mass of Semiconductor Material

The maximum removal efficiency was achieved using 0.5 g and 0.8 g of TiO₂-Dt with dilution concentrations of 60% and 40% BTEX, respectively. Increasing the mass beyond this point decreases process efficiency as the system reaches saturation equilibrium. **Table 2** presents the results.

By determining the optimal semiconductor mass for maximum efficiency, other process parameters could be optimized, and BTEX removal evaluated more effectively.

Table 2. The synthesis rate TiO₂/Dt, the total TiO₂-Dt mass and the removal efficiency, measured at λ 268 nm after 120min.

TiO ₂ /Dt Mass 9.0 (g)	BTEX Percentage (%)	Removal (%)
0.8	40	84.96
1.0	40	78.97
1.2	40	75.00
1.2	40	74.00
0.5	40	71.37
1.3	40	70.91
1.5	40	70.43
TiO ₂ /Dt Mass 6.0 (g)	BTEX Percentage (%)	Removal (%)
1.5	60	70.43
0.5	60	88.33

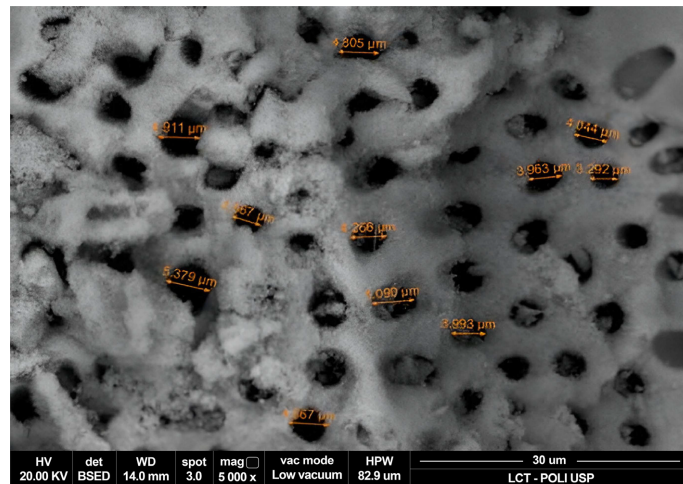
Source: Author.

3.2. Characterization of TiO₂-Diatomite

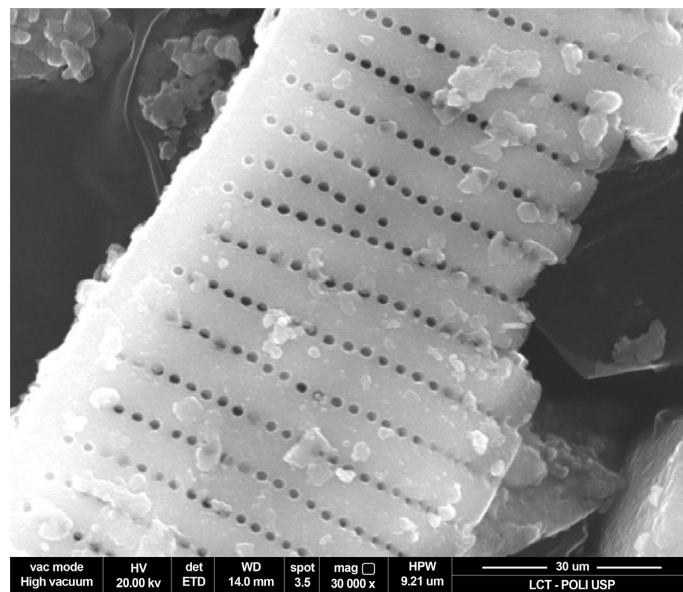
The synthesis of titanium dioxide with diatomite was carried out in the laboratory under controlled conditions. Later, the synthetic material was subjected to

exploratory photodecomposition tests and physical-chemical characterization using SEM and thermogravimetry analytical methods.

The Scanning Electron Microscope contains a source that generates an electron beam continuously fired at the sample during the test. The beam scans the sample's surface and generates high-definition images, as in **Figure 6(a)** and **Figure 6(b)**.



(a)



(b)

Figure 6. (a) SEM of synthesized TiO₂-Dt with 5.000x; (b) SEM of the synthesized TiO₂-Dt with 30.000 x. Source: Author.

The images generated by the SEM allow for different types of analyses on polymers, both structural and chemical.

Morphological information can be obtained in relation to structural analyses, such as the orientation and quality of the reinforcing fiber interface, the interface between the matrix and dispersed phase of immiscible blends, and the presence of

impurities, bubbles, cracks, and irregular surfaces.

Thermogravimetric analysis (**Figure 7**) verifies a substance's thermal degradation, thus determining its thermal stability and best drying temperature.

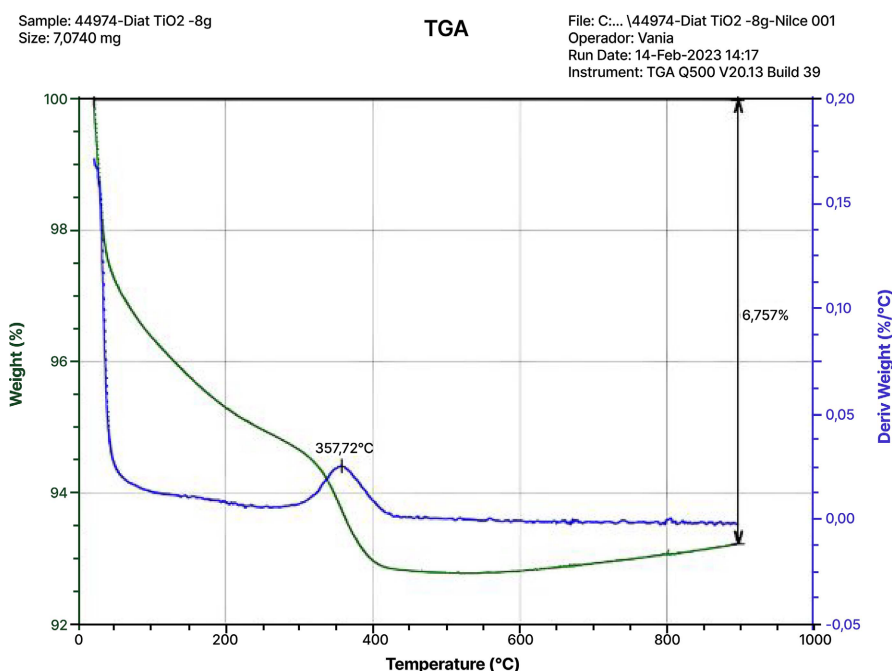


Figure 7. Thermogravimetry of the synthesized TiO_2 -Diatomite. Source: Author.

The heating ramp varied between 273 and 1123 K, observing the variability of the semiconductor mass. From 873 K, there was a loss of 93.3% of the mass value compared to the initial value of 7.1 mg, and this is due to the use of diatomite with greater volatility as a structuring agent.

TiO_2 -Dt dried in an oven at 373 K, and the material did not undergo calcination. Therefore, water and volatile compounds formed during the reaction evaporated, leaving a diatomite residue contributing to its synergistic effect during photodecomposition.

The x-ray diffractometry analysis confirmed the crystalline structure of TiO_2 -Dt prepared with 0,05 g of diatomite used in the experiments, as the TiO_2 anatase. The diffraction pattern of the TiO_2 -Dt material displayed diffraction peaks at $2\theta = 25.3, 37.9, 47.9, 54.1, 62.6, 68.9, 69.7, 75.0$, and 82.5 (**Figure 8**).

The analyzed TiO_2 -Dt sample indicated higher TiO_2 crystallinity due to the small amount of Dt added during the material's synthesis.

3.3. Infrared Analysis of TiO_2 -Dt before and after the Process

The infrared analysis of the synthesized photocatalysts shows that the characteristic silica peaks remain unchanged before and after the photodecomposition process (**Figure 9**).

Conversely, the peaks near 3500 cm^{-1} are significantly increased in the saturated photocatalyst samples (**Figure 10**).

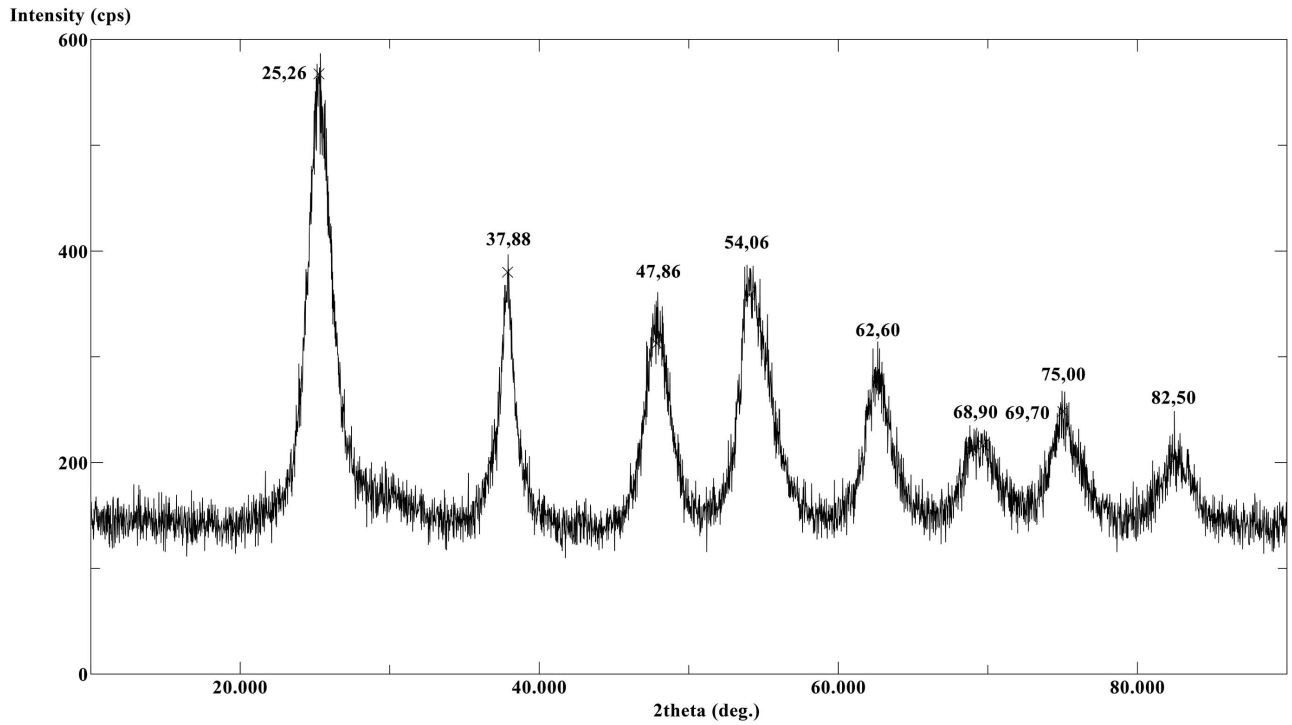


Figure 8. X-ray diffractometry of $\text{TiO}_2\text{-Dt}$ samples—Anataze. Source: Author.

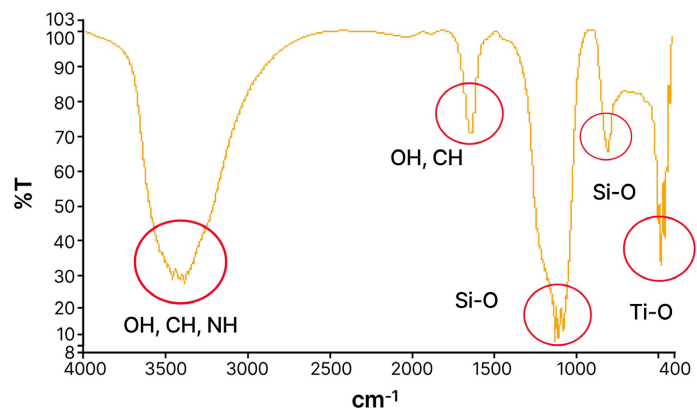


Figure 9. $\text{TiO}_2\text{-Dt}$ Spectrum before the process. Source: Author.

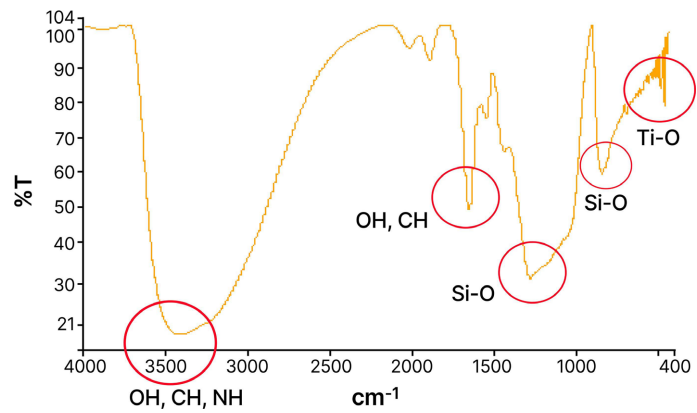


Figure 10. Spectrum of Saturated $\text{TiO}_2\text{-Dt}$, after the process. Source: Author.

Nevertheless, the structural peaks of the Si-Ti bond remain the same.

3.4. Chemical Analysis of the Photocatalysts

As shown in **Table 3**, the silica composition represents the photocatalyst's micro-structural stability, the titanium oxide composition indicates the semiconductor's efficiency in photocatalysis, and the loss on ignition reflects the biochar's thermal instability with potential structural changes after heating.

Table 3. Chemical composition of the synthesized photocatalysts.

Photocatalysts TiO ₂ -Dt	(%)
Na ₂ O (%)	0.03
MgO (%)	0.05
Al ₂ O ₃ (%)	3.81
SiO ₂ (%)	62.7
P ₂ O ₅ (%)	0.04
SO ₃ (%)	0.06
Cl (%)	<0.01
K ₂ O (%)	0.10
CaO (%)	0.17
TiO ₂ (%)	27.1
MnO (%)	nd
Fe ₂ O ₃ (%)	0.45
Co ₃ O ₄ (%)	0.76
NiO (%)	nd
CuO (%)	nd
ZnO (%)	<0.01
SrO (%)	<0.01
ZrO ₂ (%)	0.03
Loss on Ignition (%)	4.65

0.01%—XRF quantification limit; nd—not detected; Source: Author.

3.5. Photodecomposition Process

The adsorption tests were controlled by measuring benzene concentrations by spectrophotometric determination based on a calibration curve prepared with standard solutions. The concentration measurements of the complexes formed carried out with the aid of a UV-visible spectrophotometer device.

An Experimental Design matrix used the process parameters: the mass ratio between the initial concentration of benzene solutions and the mass of diatomite doped with TiO₂, the system's pH values, and the temperature of the adsorption process.

The results allowed the construction of the benzene concentration variation curves in solutions at different percolation time intervals. Determining the best photodecomposition conditions, the system's equilibrium concentration, saturation times, and the influence of pH and temperature.

Some photodecomposition processes were accomplished by changing the initial concentrations of BTEX and studying the effect of adding different masses of the semiconductor (TiO₂ Diatomite) at different intervals for 2 hours.

The tests with 60% BTEX and 40% H₂O with a mass of 1.0 g of diatomite TiO₂ presented satisfactory results, as shown in **Table 4**.

Table 4. Semiconductor total mass, initial BTEX percentage and respective removals.

Semiconductor TiO ₂ - Dt (g)	Percentage BTEX (%)	Removals (%)
0.5	60	88.3
1.5	60	70.4
0.8	40	85.0
1.0	40	75.0
1.0	40	73.0

Source: Autor.

The results indicate that moderate amounts of catalyst, such as 0.5 g to 1.5 g, are more effective for BTEX removal, while larger amounts may decrease efficiency of the photodecomposition reaction.

3.6. Boltzmann Sigmoidal Calculations for TiO₂-Dt

The experimental results showed better correspondence with Boltzmann sigmoidal curve, **Figure 11**. The calculation of the different mass of TiO₂-Dt, and BTEX percentages under laboratory conditions with artificial light for the photocatalytic decomposition process. The equation corresponds with $Qui^2 = 12.00$ and $R^2 = 0.824$.

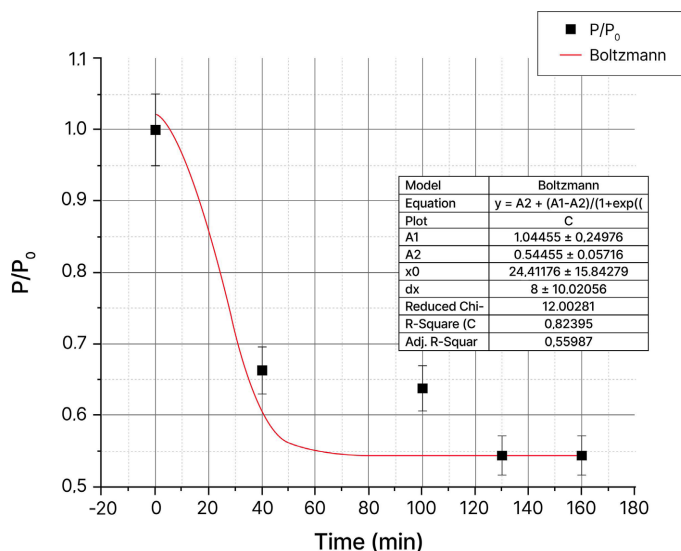


Figure 11. Boltzman equation for the experiment with 1.0 g TiO₂-Dt and 60% BTEX. Source: Author.

3.7. Thomas Model Calculations

Figure 12 shows the result of the Thomas model calculation.

The Thomas calculation, used to model the performance of contaminant photodecomposition, evaluates the BTEX removal capacity of catalytic materials.

In the tests with TiO₂-Dt and the initial 40% BTEX, the Thomas calculation revealed efficient photodecomposition, especially with 1.2 g of TiO₂-Dt, which demonstrated an increase in adsorption capacity due to the higher catalyst mass, providing effective removal, although there was no proportional increase in performance with higher masses.

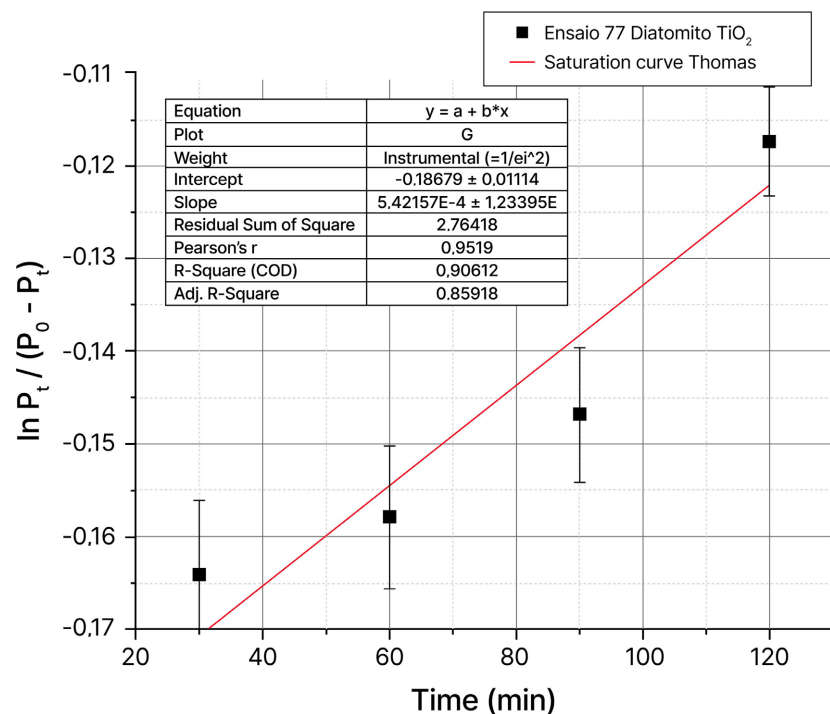


Figure 12. Thomas model calculation for test 77 with 1.2 g TiO₂-Dt and 40% BTEX. Source: Author.

In summary, the Thomas calculations showed that BTEX removal efficiency was mainly influenced by the amount of TiO₂-Dt and the BTEX percentage. The 60% BTEX demonstrated better performance with TiO₂-Dt, particularly when higher masses of TiO₂-Dt were used. The R² = 0.952 indicate high correspondence with Thomas model.

3.8. Yoon-Nelson Model Calculations

The Yoon-Nelson calculation indicated efficient adsorption performance, with short breakthrough times and efficient removal capacity. **Figure 13** shows the result of the Yoon-Nelson model calculation. The R² values of 0.869 indicate some correspondence with the model; more experimental data's will improve the R² values.

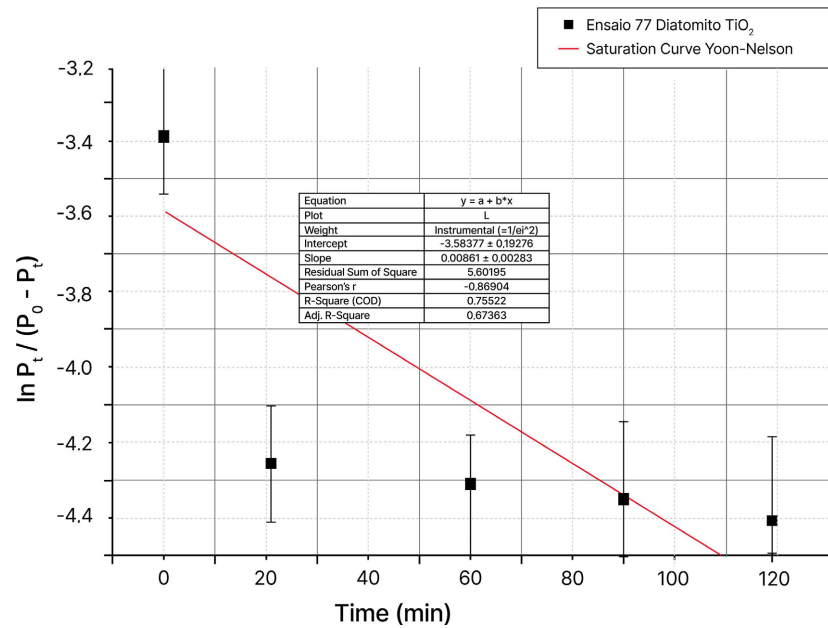


Figure 13. Yoon-Nelson model calculation for test 77 with 1.2 g TiO₂-Dt and 40% BTEX. Source: Author.

Table 5 presents the comparison of the Thomas (K_{Th}) and Yoon-Nelson (K_{YN}) constants. The literature values and those obtained in this study, allows the visualization of the contaminant removal rates across different studies.

Table 5. K_{Th} and K_{YN} values obtained in the literature and in this study.

REFERENCE	THOMAS CONSTANT - K_{Th} (ml/mg/h)	YOON-NELSON CONSTANT - K_{YN} (1/min) 10^{-5}
In this study	From 0.0092 to 7.76	From 0.0016 to 5.42
El-Aswar, E.I., Ibrahim, S.S., Abdallah, Y.R., & Elsharkawy, K. (2024) Removal of ciprofloxacin and heavy metals from water by bentonite/activate carbon composite: Kinetic, isotherm, thermodynamic and breakthrough curve modeling studies. Journal of molecular liquids 403.	From 0.055 to 3.54 Depending on the bed height, flow rate, and initial concentration	From 0.0091 to 0.0134 Depending on the bed height, flow rate, and initial concentration
Lv, N. Li, X. Phosphorous removal from wastewater using Ca modified attapulgite: fixed bed column performance and breakthrough curves analysis. Journal of Environmental Management (2023) 328.	From 0.083 to 0.36	From 0.086 to 0.11

Source: Author.

Comparing the values obtained in this study with those presented in the literature, it is observed that they are of the same order of magnitude, although with a wider range of variation. This indicates that the parameters of the photodecomposition process are efficient, can be used and can still be improved and stabilized.

3.9. GC-MS Chromatography Tests

GC-MS chromatography analyses of synthetic water contaminated with initial 60% of BTEX identify the characteristics BTEX peaks in the beginning of the photodecomposition process (A) and after 2 h (B). **Figure 14** shows the results with the retention time characteristics of benzene, toluene, ethylbenzene, and xylene compounds, after 2h there was no detectable contamination of BTEX, or there was about 100% of removal.

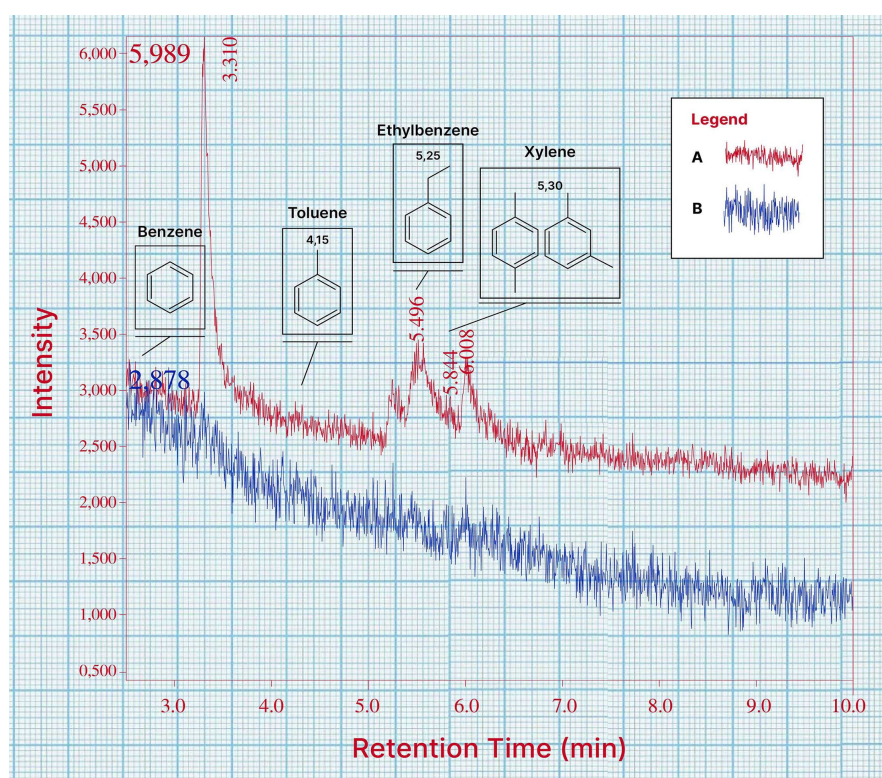


Figure 14. Chromatography analysis of the initial aqueous solution of BTEX (A) and after 2h of photocatalytic decomposition (B). Source: Author.

The optimization of the solar photocatalytic decomposition process offers a promising alternative for treating groundwater contaminated with BTEX. The results showed that TiO_2 microstructured with diatomite could remove up to 100% of BTEX from contaminated water. Additionally, the process allows for the recovery of leaked fuel from gasoline tanks by simply organic phase separation. The photocatalytic decomposition tests indicated that solar radiation is essential for the complete degradation of BTEX. The solar photocatalysis is crucial for the total removal of contaminants.

The TiO_2 -Dt and solar photocatalysis proved an effective strategy for contaminated water remediation, offering a sustainable and accessible solution. The thermogravimetric analysis confirmed the stability of the photocatalyst, highlighting its importance for process efficiency.

The developed system is applicable in both open and closed areas, and field tests

using natural solar radiation prove its effectiveness. Considering an open area the Solar energy can also power the system, making the photocatalyst system autonomous and cost-effective. Based on such promising results, there is a suggestion to implement a pilot system at a gas station contaminated site to evaluate the results on-site.

Optimizing the photodisinfection process can provide a new alternative also to the disinfection methods used in the country.

The results demonstrated that up to 100% of BTEX can be removed from BTEX contaminated water using TiO_2 microstructured with diatomite. In the process under study, it is still possible to recover the fuel leaked from the tanks and reuse it after organic phase separation.

4. Conclusion

The results confirm the use of diatomite as biotemplate and TiO_2 , prepared from the hydrolysis of titanium isopropoxide and microstructured, resulted in a material with exceptional properties for use as a semiconductor in solar photocatalytic decomposition processes. Through various tests, it was possible to optimize the parameters of the solar photocatalytic decomposition process, achieving complete (100%) removal of BTEX compounds from contaminated water.

The results demonstrate the feasibility and efficiency of using solar photocatalytic decomposition to treat contaminated groundwater with BTEX. This process was effective in removed and proved to be a sustainable solution, in line with the growing need to treat and preserve the surface and underground water quality. Promoting solar photocatalytic decomposition could represent a practical and environmentally friendly alternative for treating gasoline-derived contamination.

Additionally, the photocatalytic decomposition tests significantly improved BTEX removal from contaminated water. Solar radiation played a key catalytic role, accelerating the photocatalytic degradation of compounds on TiO_2 -Dt surface. Samples exposed to solar radiation exhibited a faster and more efficient reduction of BTEX levels, highlighting the importance of photocatalysis as an essential complement to water treatment processes.

Future research could focus on optimizing the TiO_2 -Dt composite by exploring alternative synthesis methods, evaluating its performance with other organic pollutants, and testing its scalability in real-world scenarios. Investigating the long-term stability and reusability of the catalyst, as well as the integration of solar photodecomposition with other water treatment technologies, would further enhance its applicability and impact in groundwater remediation.

Acknowledgments

Mr. Takashi and João Evangelista, Woodworking and Electrical Technician of the Chemistry and Environment Control Center at the Institute for Nuclear and Energy Research, for assisting in constructing the solar chamber and CAPES nº 88887.757078/2022-00.

Conflicts of Interest

The authors declare no conflicts of interest regarding the publication of this paper.

References

- (2000). CONAMA—Resolução no 273, de 29 de novembro de 2000. https://cetesb.sp.gov.br/licenciamento/documentos/2000_Res_CONAMA_273.pdf
- (2009) CONAMA—Resolução no 420, de 28 de dezembro de 2009. <https://cetesb.sp.gov.br/areascontaminadas/wpcontent/uploads/sites/17/2017/09/resolucao-conama-420-2009-gerenciamento-de-acs.pdf>
- Andrade, J. D. A., Augusto, F., & Jardim, I. C. S. F. (2010). Biorremediação de solos contaminados por petróleo e seus derivados. *Eclética Química*, 35, 17-43. <https://doi.org/10.1590/s0100-46702010000300002>
- ANP (2021). *Agência Nacional de Petróleo, Gás Natural e Biocombustíveis—ANP (Brasil). Brazilian Statistical Yearbook for Oil, Natural Gas and Biofuels—2021.* <http://www.anp.gov.br/conteudo-do-menu-superior/31-dados-abertos/6010-anuario-estatistico-2020-open-data>
- Buth, D. F. (2009). *Degradação fotocatalítica da tetraciclina em solução aquosa empregando TiO₂ suportado*. Ph.D. Thesis, Universidade Federal do Rio Grande do Sul.
- Companhia Ambiental do Estado de São Paulo—CETESB (2014). *List of Contaminated and Rehabilitated Areas in the State of São Paulo* (p. 14).
- Companhia Ambiental do Estado de São Paulo—CETESB (2021). *Contaminated Areas Management Manual.* <http://areascontaminadas.cetesb.sp.gov.br/manual-de-gerenciamento/>
- DATAGEO (2021). *São Paulo Environmental System.* <https://datageo.ambiente.sp.gov.br/app/?ctx=DATAGEO>
- Dias, S. P., Vaghetti, J. P., Lima, É. C., & Brasil, J. L. (2016). *Analytical Chemistry: Essential Theory and Practice*. Bookman.
- Dórea, H. S., Bispo, J. R. L., Aragão, K. A. S., Cunha, B. B., Navickiene, S., Alves, J. P. H. et al. (2006). Analysis of BTEX, PAHs and Metals in the Oilfield Produced Water in the State of Sergipe, Brazil. *Microchemical Journal*, 85, 234-238. <https://doi.org/10.1016/j.microc.2006.06.002>
- El-Aswar, E. I., Ibrahim, S. S., Abdallah, Y.R., & Elsharkawy, K. (2024) Removal of Ciprofloxacin and Heavy Metals from Water by Bentonite/Activate Carbon Composite: Kinetic, Isotherm, Thermodynamic and Breakthrough Curve Modeling Studies. *Journal of Molecular Liquids*, 403, Article ID: 124821. <https://doi.org/10.1016/j.molliq.2024.124821>
- Ferro, M. D. (2024). *Utilização de TiO₂ microestruturado com biocarvão para desinfecção solar catalítica de efluentes contaminadas por microrganismos*. Ph.D. Thesis, Instituto de Pesquisas Energéticas e Nucleares, IPEN. <http://repositorio.ipen.br/>
- Kotani, O. P. (2023). *Utilização do TiO₂-Diatomito em processos de fotodesinfecção em águas contaminadas por bactérias*. Ph.D. Thesis, Instituto de Pesquisas Energéticas e Nucleares, IPEN-CNEN. [http://repositorio.ipen.br/\(01/10/2024\)](http://repositorio.ipen.br/(01/10/2024))
- Luiz, A. M. (1985). *How to Take Advantage of Solar Energy* (p. 191). Editora Edgard Blücher Ltda.
- Ortiz, N., Silva, A., Lima, G. N. S., & Hyppolito, F. P. (2018). Using Solar-TiO₂ and Biocarbon to Decompose and Adsorb Amoxicillin from Polluted Waters. *International Journal of Chemistry*, 10, 131-136. <https://doi.org/10.5539/ijc.v10n1p131>

- Ray, S. K., Dhakal, D., Kshetri, Y. K., & Lee, S. W. (2017). Cu- α -NiMoO₄ Photocatalyst for Degradation of Methylene Blue with Pathways and Antibacterial Performance. *Journal of Photochemistry and Photobiology A: Chemistry*, 348, 18-32. <https://doi.org/10.1016/j.jphotochem.2017.08.004>
- Suri, R. P. S., Liu, J., Hand, D. W., Crittenden, J. C., Perram, D. L., & Mullins, M. E. (1993). Heterogeneous Photocatalytic Oxidation of Hazardous Organic Contaminants in Water. *Water Environment Research*, 65, 665-673. <https://doi.org/10.2175/wer.65.5.9>
- Vazzoler, A. (2019). *Cálculo de reatores catalíticos gássólido. Volume 1.*